VOL. 12, NO. 8, APRIL 2017 ISSN 1819-6608
ARPN Journal of Engineering and Applied Sciences

www.arpnjournals.com

PRELIMINARY NUMERICAL SIMULATION OF STEADY-STATE GAS-LIQUID FLOW IN HORIZONTAL T-JUNCTION

Ban Sam[1], William K. S. Pao[1], Mohammad S. Nasif[1] and Titus Ntow Ofei[2]
[1]Mechanical Engineering Department, Universiti Teknologi Petronas, Bandar Seri Iskandar, Perak, Malaysia
[2]Petroleum Engineering Department, Universiti Teknologi Petronas, Bandar Seri Iskandar, Perak, Malaysia
E-Mail: William.Paokings@petronas.com.my

ABSTRACT

T-junction, or commonly known as stand pipe appendage, is used by oil/gas industries to tap gas from existing production header for the purpose of downstream pipeline instrumentation. The appendage is either pre-design or retro fitted with minimum internals for maximum reliability for remote deployment. The motivation for this research originated from the lack of stand-pipe design method to correctly account for the splitting/separation nature of multiphase fluid within the pipeline straight from the production header. Consequently, a certain amount of liquid migrates together with the gas, resulting in the so-called carryover issue. This situation is further aggravated by the different flow regimes in the header pipeline which is not taken into account by the design practice. The negative consequences of this carryover on the operation of downstream unit have often led to frequent trip and maintenance issues. Therefore, understanding the behavior of gas-liquid flow through T-junction is essence on optimizing the gas phase separation. This study aims to examine the effect of phase volume fraction on the separation of gas-liquid in a T-junction pipe. A computational fluid dynamics (CFD) simulation by means of ANSYS-CFX is employed to model and solve the fundamental mass, momentum and turbulent equations. The computed solutions are compared with experimental data and a satisfactory agreement is achieved. Results show that the gas separation efficiency increases as the initial gas volume fractions increases.

Keywords: two-phase flow, gas-liquid flow, t-junction.

INTRODUCTION

Gas-liquid two-phase flow in pipes is a common occurrence in the petroleum industry production and transportation of oil and gas. Accurate prediction of the flow pattern, pressure drop and liquid holdup is imperative for the design of production, transport systems and for maintenance and operation of the downstream facilities. Two-phase flow presents a complex flow configuration. Flow behavior is a function of flow variables such as gas and liquid flow rates, pipe diameter, inclination angle and fluid properties (gas and liquid density, viscosities and surface tension)[10]. In the petroleum industry application, phase separation in T-junctions has been observed as early as 1973 by Oranje [23]. Oranje noticed that condensate in gas lines did not appear equally at all terminal points on branched pipelines.

The most useful methods of representing the phase split data is a plot of the fraction of the inlet liquid diverted into the branch arm against the fraction of the inlet gas diverted into the same branch. By calculation, the fraction of gas taken off and the fraction of liquid taken off could be obtained based on the following formulas [1-6]:

$$\text{Gas taken off} = \frac{\text{Gas mass flow rate of side branch } (\dot{m}_{g3})}{\text{Gas mass flow rate of inlet } (\dot{m}_{g1})} \quad (1)$$

$$\text{Liquid taken off} = \frac{\text{Liquid mass flow rate of side branch } (\dot{m}_{l3})}{\text{Liquid mass flow rate of inlet } (\dot{m}_{l1})} \quad (2)$$

According to Wren, Baker and Baker *et al.,* there are many physical factors and dominant forces that affect how the two-phase flow approaching the junction may be divided between the outlets. These are considered to be gravity, inertia and pressure [4][5][18].

Altering the orientation of the side arm will influence the phase separation as it will change the orientation of the gravitational force acting on the fluid [18]. Studies [1][4]have concluded that when the side arm is oriented vertical upward pointing 12 o'clock, more gas is found in the side arm. At 3/9 o'clock, phase splitting is equal and when the side arm is oriented vertically downward at 6 o'clock, more liquid is discovered at the side arm.

Conte and Azzopardi [7], studied experimentally the division of gas/liquid flow at a large diameter T-junction. The separation of the phases has been quantified for horizontal semi-annular flow. Film thickness variations about the circumference of the inlet and outlet pipes have been obtained using conductivity techniques. In addition, liquid depth profiles within the junction have been measured. It has shown that the phase split of semi-annular flow at a large diameter T-junction is liquid dominated with less than 20% of the liquid is taken off for 80% gas take off.

Das *et al.,* [8], reported a study of phase split at a horizontal T-junction with main and side branches of 5 mm in diameters. The results were compared with those reported for larger T-junctions. The authors observed that, the side arm take-off tends to be richer in the gas phase with increase in pressure under all flow conditions. The reason has been attributed to the complex effect of pressure on the interface position which in turn determines the gas and liquid momentum.

Yang and Azzopardi [19] provided data on the split of liquid/liquid two-phase flow at a horizontal T-junction with equal pipe diameters, horizontal main pipe

and side-arm. According to the authors there is little phase separation and hence this configuration of T-junction would not be efficient as a partial separator.

In horizontal T-junction, the associated pressure drop along the side arm and axial distance available for take-off into the side arm will be altered by the reduced side arm diameter (reduced T-junction) [4][14][18].

Further studies compared the pressure drops for both regular and reduced horizontal T-junction with similar inlet flow rates [4][17][18]. The pressure drop between the inlet and the run arm is relatively small and unaffected by the diameter of the side-arm. However, the inlet to side-arm pressure drop increases significantly with a decrease in the side-arm diameter ratio. So, for the same inlet conditions, a higher pressure drop is associated with the reduced T-junction. This is due to the higher gas velocities within the reduced diameter pipe for the same mass fraction extracted through the branch, as demonstrated by Bernoulli's equation.

Hong [10] studied the effect of liquid viscosity on the phase separation in horizontal T-junction where the viscosity of the liquids were 1 cP for water and 5 ~ 10 cP for mixture of water and hydroxyethyl cellulose. Results showed that the amount of liquid diversion into the side arm increased with increasing of liquid viscosity and this scenario can be explained by using the inertial and centripetal forces theory.

They explained that the velocity of the liquid flow was decreased as the liquid viscosity increased for the fixed inlet of gas velocity. Thus, the low liquid velocity will have lower inertial effect on the liquid. At the same time, the two phase flow through the T-junction will be subjected to the centripetal force due to the existing bending corner. The effect of the centripetal force will remain constant and unaffected by the liquid viscosity. Hence, for the fixed value of inlet gas velocity and increasing of liquid viscosity, the centripetal force will overcome low liquid inertial in order to draw more liquid into the side arm.

Brito *et al.,* [6] studied the effect of medium oil viscosity on two-phase oil-gas flow behavior in horizontal pipes, experimental program on medium oil viscosities (39 cP< μ_{oil} <166 cP). The experiments are performed using a flow loop with a test section of 50.8-mm ID and 18.9-m-long horizontal pipe. The range of superficial liquid and gas velocity are 0.01 m/s to 3.0 m/s and 0 to 7.0 m/s, respectively. The existing flow patterns: stratified smooth, stratified wavy, elongated bubble, slug, dispersed bubble and annular, were observed for the studied flow conditions. Most of the experimental points observed in this study correspond to slug flow. The stratified smooth region decreases when the oil viscosity increases. Liquid viscosity increase delays the formation of an eddy at the liquid slug front, thus increasing the region of the elongated bubble flow. Gas bubble entrainment in the elongated bubble region increases when oil viscosity increases. For the lower oil viscosities (39 cP and 60 cP), transition from intermittent flow to dispersed bubble flow occurs at higher superficial gas velocities in comparison with higher oil viscosities (108 cP and 166 cP). Annular flow was only observed for the highest oil viscosity (166 cP).

Studies have shown that the flow pattern approaching T-junction would affect the phase separation [4][5][18]. The type of flow pattern in the pipe is dependent on the superficial velocity of gas and liquid. The effect of the flow pattern onto the phase separation in vertically upward and downward T-junction was firstly noticed that the flow at the top section of the pipe would be influenced by the vertical upward side arm.

This paper is to put forward a general three-dimensional, two-fluid numerical model and present its application to two-phase dispersed bubbly flow through a T-junction with round cross-sections, and to study the effect of phase volume fraction on the separation of gas-liquid in a T-junction pipe. The experimental data of Davis and Fungtamasan [9]are used to make comparisons for validation purpose.

METHODOLOGY

Numerical methods

The present model solves full steady-state three-dimensional, two-fluid transport equations, where both phase are treated as interpenetrating continua distinguished by a volume fraction factor in the Eulerian frame. Turbulence is described by the standard $k-\varepsilon$ model. The detailed governing equations are presented below. There are other models such as VOF and mixture, however, VOF model is appropriate for stratified or free-surface flows, and the mixture and Eulerian models are appropriate for flow in which the phases mix or separate and/or dispersed-phase volume fractions exceed 10%. The mathematical model used to describe the multiphase flow is the Eulerian-Eulerian inhomogeneous model [4][11][18]. In this case, the governing equations are:

1. Continuity equation

By assuming isothermal flow condition, the fluid phase continuity equation of phase $q$can be expressed as follows:

$$\frac{\partial}{\partial t}\left(\alpha_q \rho_q\right)+\nabla\cdot\left(\alpha_q \rho_q \vec{v}_q\right)=\sum_{p=1}^{n}\left(\dot{m}_{pq}-\dot{m}_{qp}\right)+S_q \quad (3)$$

2. Momentum equation

The interaction of inter phase momentum transfer between each phase can be described as follows:

$$\frac{\partial}{\partial t}\left(\alpha_q \rho_q \vec{v}_q\right)+\nabla\cdot\left(\alpha_q \rho_q \vec{v}_q \vec{v}_q\right)=-\alpha_q \nabla p+\nabla\cdot\bar{\bar{\tau}}_q+\alpha_q \rho_q \vec{g}$$
$$+\sum_{p=1}^{n}\left(K_{pq}\left(\vec{v}_p-\vec{v}_q\right)+\dot{m}_{pq}\vec{v}_{pq}-\dot{m}_{qp}\vec{v}_{qp}\right)$$
$$+\left(\vec{F}_q+\vec{F}_{lift,q}+\vec{F}_{wl,q}+\vec{F}_{vm,q}+\vec{F}_{td,q}\right) \quad (4)$$

Where q and $p$represent any two phases, $\propto_q$=volume fraction, ρ =density, $\vec{v}_q$ = velocity of phase,

$\dot{m}_{pq}$ =mass transfer of a p phase to a$q$phase,$\dot{m}_{qp}$ = mass transfer of a q phase to ap phase,S_q = generation of mass for the q phase, n = number of phase of the flow, p= pressure shared by all phases, $\bar{\bar{\tau}}_q$ = tensor of viscous stresses of phase q, $\vec{g}$ =gravitational acceleration, K_{pq} =interaction force between phase, $\vec{v}_{qp}$ = phase relative velocity, $\vec{F}_q$ = external body force, $\vec{F}_{lift,q}$ =lift force, $\vec{F}_{vm,q}$ = virtual mass force, $\vec{F}_{wl,q}$ =wall lubrication force and $\vec{F}_{td,q}$ = turbulent dispersion force.

Figure-1 shows a schematic diagram of T-junction model with horizontal main arm (inlet), horizontal run arm (outlet) and vertical upward side arm which are defined by subscript 1, 2, and 3 respectively. The division of two phases at T-junction depends on many variables including the geometries (i.e. variation in length, radius curvature, diameter of each arm and variation in angle) and operating conditions (i.e. superficial velocity, viscosity and density and mass split ratio of the two outlets).

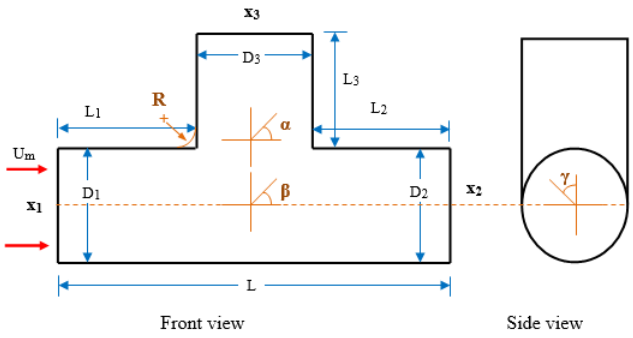

Figure-1. Schematic diagram of T-junction.

A two phase mixture enters through the main arm with a liquid and gas mass flow rate of $\dot{m}_{l1}$ and$\dot{m}_{g1}$. At the T-junction, inlet mass flow rate, $\dot{m}_1$will split into run arm and side arm which are defined as mass flow rate of $\dot{m}_2$ and $\dot{m}_3$ respectively. The two phase mixture in run arm consists of $\dot{m}_{l2}$ and $\dot{m}_{g2}$ and similarly the two phase mixture in side arm consists of $\dot{m}_{l3}$ and$\dot{m}_{g3}$. The following equations will be used in presenting percentage of gas going into the side arm

Overall mass flow rate:$\dot{m}_3 = \dot{m}_{l3} + \dot{m}_{g3}$ (5)

Overall mass split ratio at side arm:$x_3 = \dot{m}_3/\dot{m}_1$ (6)

Gas taken off: $F_{g3} = \dot{m}_{g3}/\dot{m}_{g1}$ (7)

Liquid taken off:$F_{l3} = \dot{m}_{l3}/\dot{m}_{l1}$ (8)

Numerical simulation

The CFD simulation used in this paper utilizes CFX solver from ANSYS Inc. For geometry and mesh generation, the ANSYS software ICEM CFD was used. ICEM CFD is a meshing software. It allows for the use of CAD geometries or to build the geometry using a number of geometry tools. In ICEM CFD a block-structured meshing approach is employed, allowing for hexahedral meshes also in rather complex geometries. Both structured and unstructured meshes can be created using ICEM CFD.

In CFX, only the coupled solver is implemented and the vertex based Finite Volume Method (FVM) approach is used for discretisation. Two main multiphase model are available; a homogeneous and an inhomogeneous model. The homogeneous corresponds to a Volume of Fraction (VOF) model. The inhomogeneous model is based on the Euler-Euler approach and can be used together with several subsidiary models to model dispersed flow, mixtures of continuous fluids etcetera. In this study the inhomogeneous model was adopted where the liquid was modelled as continuous fluid, whereas, the gas bubbles were modelled as dispersed fluid. A gas bubble size of 2mm was chosen to model the dispersed gas bubble size as also predicted by Davis and Fungtamasan [9]in their experiment.

In CFX, the same discretisation methods are available for all transport equations, including the volume fraction equation. A first order scheme, a blending scheme and a higher resolution scheme are available. Depending on the types of phases, for example continuous or dispersed fluid, different inter phase transfer models are made available.

Meshing, boundary conditions and validation

The domain and the meshing were created using ANSYS ICEM CFD. Three domains were created with dimensions taken from the experimental setup of Davis and Fungtamasan [9], a mixture of water and air bubbly flow was introduced into a T-junction. Table-1 presents the input parameters used in validating the simulation model.

Table-1. Input parameter for validation [9].

Input parameters	
Diameter, D_1, D_2 and D_3 (mm)	50
Length, L_1, L_2 and L_3 (mm)	500
Liquid density, ρ_l (kg/m^3)	998.2 (water)
Gas density, ρ_g (kg/m^3)	1.225 (air)
Initial gas saturation, α_g	0.47, 0.52, 0.56, 0.63
Inlet mixture velocity, U_m (m/s)	2.92, 6.21, 5.57, 6.62
Angle of side arm, γ (°)	90
Overall mass split ratio, Q	0.2, 0.4, 0.6, 0.8
Operating pressure, $P(kPa)$	101.325
Averaged bubble diameter, (mm)	2

Mesh expansion factor measures the magnitude of the rate of change of the adjacent element areas or volumes. The mesh aspect ratio is determined by dividing the smallest element edge length by the largest, usually they must be less than 100, however it is expected and accepted that mesh aspect ratio within the boundary layer will be of the magnitude 10^5-10^6. Table-2 shows the ICEM and ANSYS CFX criteria to determine the acceptable mesh quality for CFX solver.

Table-2. CFX ICEM criteria to determine acceptable mesh quality for CFX Solver.

Key Factor	Requirement	Base mesh Value
Minimum volume	> 0	1.22×10^{-13}
Minimum determinant	> 0.2	0.37
Minimum angle	Preferably> 18,definitely> 9	17.28

Negative volumes or determinants indicate an inverted element and ANSYS CFX solver will not run.

The discretization of the three-dimensional (3D) domain resulted in approximately 441345 total number of nodes and 457698 total number of elements. The distribution of cells at the side arm and around the junction can be seen in Figure-2.

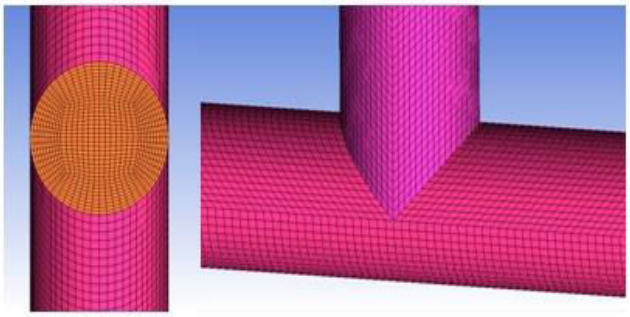

Figure-2. To the left: Element distribution at side arm. To the right: Zoom of mesh in vicinity of the junction.

RESULTS AND DISCUSSIONS

Flow parameters of four inlet flow conditions are investigated and analyzed in this section, where each flow condition consists of four groups of overall mass split ratio. Apart from the flow split results, the present model is able to give a more insight for the fluid flow nature, where the the fraction of gas taken off and the fraction of liquid taken off are presented.

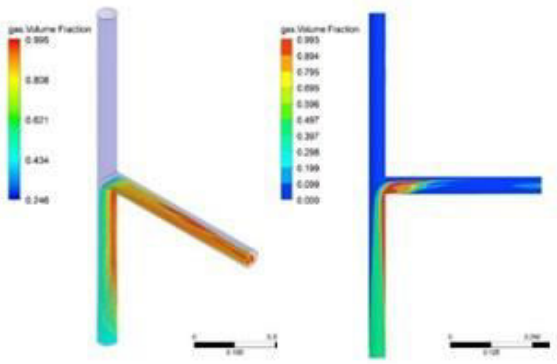

Figure-3. Contour plots of gas volume fraction 3D streamline and on mirror plane z = 0 at horizontal T-junction with the flow condition 1: U_m = 2.92m/s &α_g = 0.47.

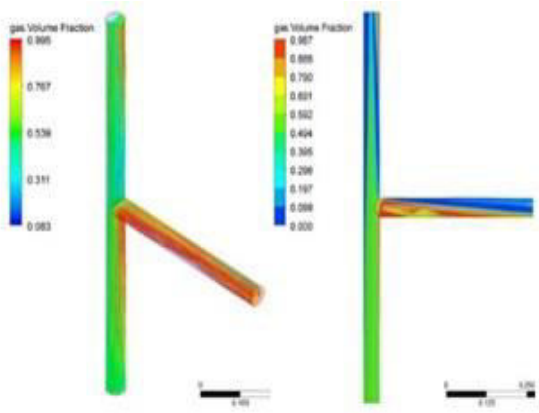

Figure-4. Contour plots of gas volume fraction 3D streamline and on mirror plane z = 0 at horizontal T-junction with the flow condition 2:U_m = 6.21m/s &α_g = 0.52.

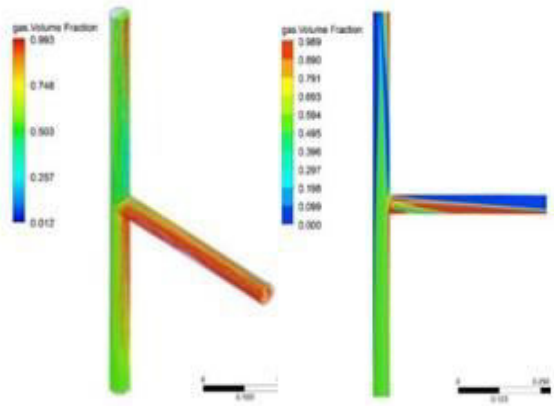

Figure-5. Contour plots of gas volume fraction 3D streamline and on mirror plane z = 0 at horizontal T-junction with the flow condition 3:U_m = 5.57m/s &α_g = 0.56.

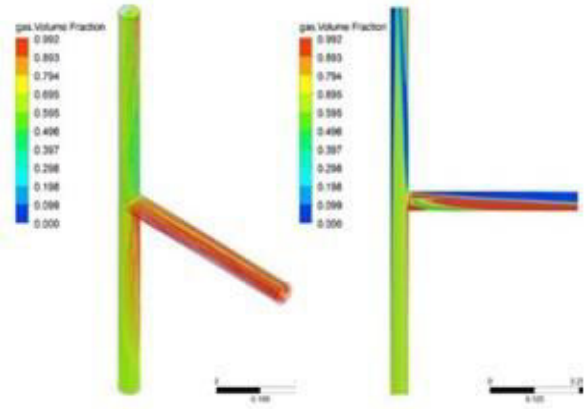

Figure-6. Contour plots of gas volume fraction 3D streamline and on mirror plane z = 0 at horizontal T-junction with the flow condition 4:U_m = 6.62m/s &α_g = 0.63.

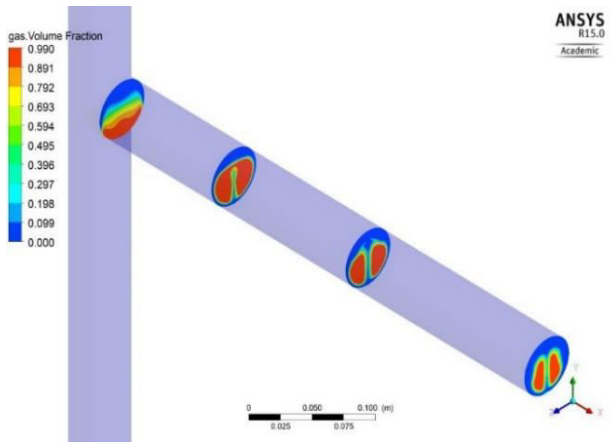

Figure-7. Contour plots of gas volume fraction at planes located at x = 0.1, 0.2, 0.3, and 0.4 in the side arm with the flow condition 1:U_m = 2.92m/s &$\alpha_g = 0.47$.

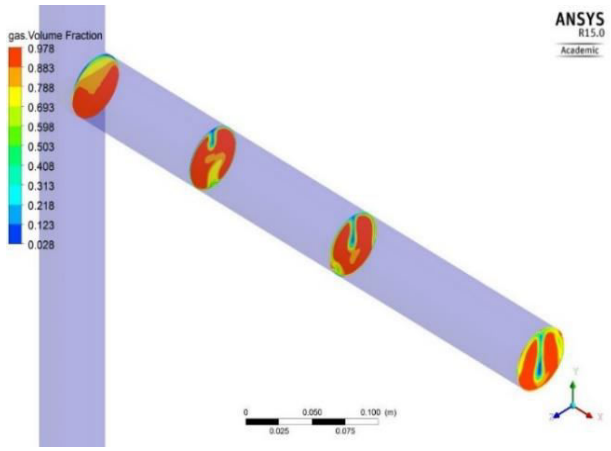

Figure-8. Contour plots of gas volume fraction at planes located at x = 0.1, 0.2, 0.3, and 0.4 in the side arm with the flow condition 2: U_m = 6.21m/s &$\alpha_g = 0.52$.

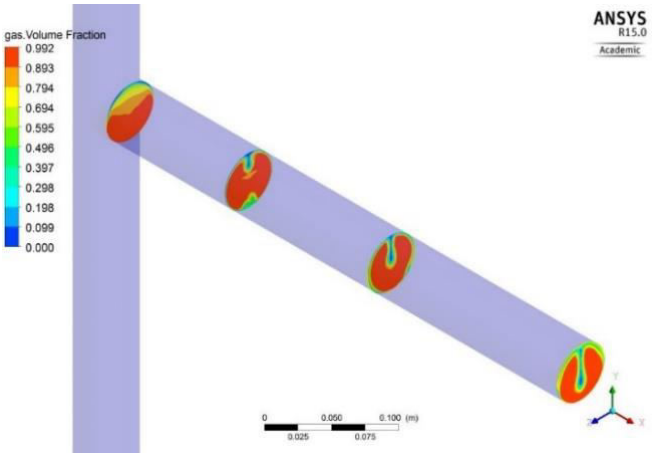

Figure-9. Contour plots of gas volume fraction at planes located at x = 0.1, 0.2, 0.3, and 0.4 in the side arm with the flow condition 3: U_m = 5.57m/s &$\alpha_g = 0.56$.

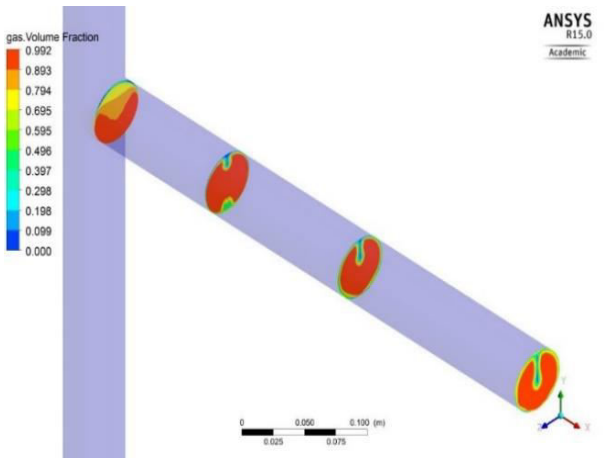

Figure-10. Contour plots of gas volume fraction at planes located at x = 0.1, 0.2, 0.3, and 0.4 in the side arm with the flow condition 4: U_m = 6.62m/s &$\alpha_g = 0.63$.

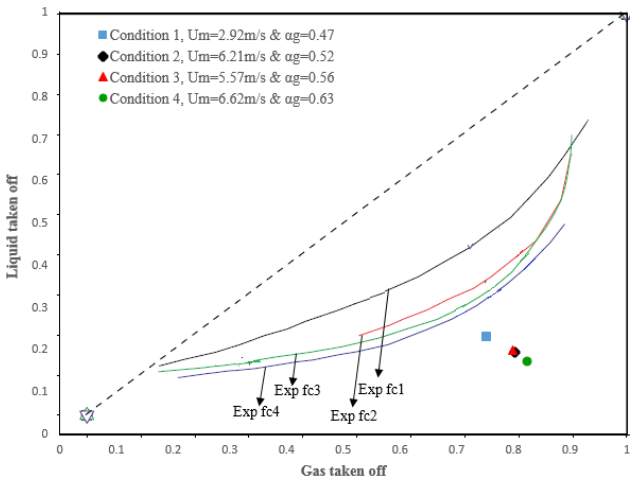

Figure-11. Simulated flow split curves compared with experimental results (d = 2 mm).

Figure-3-6 shows the views of gas volume fraction at the side arm. It can be seen that the gas runs faster than liquid in the region above the usually deemed "dividing streamline" towards the side arm, and the water flows faster in the run arm. This insight velocity analysis suggests that it is the inertia difference that results in the flow split phenomenon.

Figure-7-10 illustrates various flow patterns for gas volume fraction on the mirror plane. For flow condition 1, as shown in Figure-7, there is more liquid fraction at the side arm, however, for flow conditions 2 to 4, there are more gas at the side arm which indicates better separation in the side arm (see Figure-8-10).

Figure-11 shows the flow split results of the four flow conditions and they are compared with the experimental results. The *x*-axis is the gas taken off value defined as $\dot{m}_{g3}/\dot{m}_{g1}$ and the y-axis is the liquid taken off value, defined as$\dot{m}_{l3}/\dot{m}_{l1}$. The central line is the equal split line where the area belowsymbolizes gas rich zone, whereas the area above stands for liquid rich zone for the side arm. The calculated results of gas and liquid volume

fractions at the side arm are expressed as: flow condition 1: $F_{g3} = 0.753187$ and$F_{l3} = 0.22858$, flow condition 2: $F_{g3} = 0.802849$and$F_{l3} = 0.194919$, flow condition 3: $F_{g3} = 0.798817$ and$F_{l3} = 0.198951$, flow condition 4: $F_{g3} = 0.825763$ and$F_{l3} = 0.172005$.

CONCLUSIONS

A two-fluid Euler-Euler approach has been undertaken to investigate the phase split phenomenon in a 50mm equal diameter T-junction for bubbly flow. The following conclusions can be drawn through the cases studied above.

- CFD calculation using CFX and meshing with ICEM were performed to predict the air-water bubbly flow in the T-junction of [9] experiments.
- Gas phase inclines to flow into the side arm for bubbly flow, even for small extraction rate cases. A possible reason may be that the pressure difference of the side arm to inlet arm is much larger than that for the run arm. The lighter gas phase responds more easily to pressure gradient than the liquid phase for the same pressure force.
- The simulation result show that the gas separation efficiency increases as the initial gas volume fractions increases.

ACKNOWLEDGEMENTS

The authors appreciate all technical and financial support from the Universiti Teknologi Petronas (UTP), Malaysia.

REFERENCES

[1] Azzopardi B. J. 1999. The Effect of Side Arm Diameter on Phase Split at T-Junctions. Paper presented at the SPE Annual Technical Conference and Exhibition, Houston, Texas.

[2] Azzopardi B. J. 2010. Multiphase Flow Chemical Engineering and Chemical Process Technology, 1.

[3] Azzopardi B. J., and Rea S. 2000. Phase separation using a simple T-junction. Paper presented at the SPE Annual Technical Conference and Exhibition.

[4] Baker G., Clark W. W., Azzopardi B. J., Wilson J. A. 2007. Controlling the phase separation of gas–liquid flows at horizontal T-junctions. AIChE journal, 53(8), 1908-1915.

[5] Baker G. 2003. Separation and control of gas-liquid flows at horizontal T-junctions. University of Nottingham.

[6] Brito R., Pereyra E., Sarica C. 2013. Effect of Medium Oil Viscosity on Two-Phase Oil-Gas Flow Behavior in Horizontal Pipes. Paper presented at the Offshore Technology Conference, Houston, Texas, USA.

[7] Conte G, and Azzopardi B. J. 2003. Film thickness variation about a T-junction. International journal of multiphase flow, 29(2), 305-328.

[8] Das G, Das P. K., Azzopardi B. J. 2005. The split of stratified gas–liquid flow at a small diameter T-junction. International Journal of Multiphase Flow, 31(4), 514-528.

[9] Davis M. R., and Fungtamasan B. 1990. Two-phase flow through pipe branch junctions. International Journal of Multiphase Flow, 16(5), 799-817.

[10] Hong K. C. 1978. Two-phase flow splitting at a pipe tee. Journal of Petroleum Technology, 30(02), 290-296.

[11] Issa R.I., and Oliveira P. J. 1994. Numerical prediction of phase separation in two-phase flow through T-junctions. Computers & fluids, 23(2), 347-372.

[12] Liu Y., and Li W. Z. 2011. Numerical Simulation on Two-Phase Bubbly Flow Split in a Branching T-Junction. International Journal of Air-Conditioning and Refrigeration, 19(04), 253-262.

[13] Oranje L. 1973. Condensate behavior in gas pipelines is predictable. Oil Gas J, 32, 39-44.

[14] Pao W., Hashim F. M., Ming L. H. 2014. Computational Analyses of Passive Wet Gas Separation in Branched Piping. Paper presented at the MATEC Web of Conferences.

[15] Peng F., and Shoukri M. 1994. A Study of Dividing Steam-Water Flow in T-Junctions: Experiments and Analyses. McMaster University.

[16] Stacey T, Azzopardi B. J., Conte G. 2000. The split of annular two-phase flow at a small diameter T-junction. International journal of multiphase flow, 26(5), 845-856.

[17] Walters L. C., Soliman H. M., Sims G. E. 1998. Two-phase pressure drop and phase distribution at reduced tee junctions. International journal of multiphase flow, 24(5), 775-792.

[18] Wren E., and Mary K. 2001. Geometric effects on phase split at a large diameter T-junction. University of Nottingham.

[19] Yang L, and Azzopardi B. J. 2007. Phase split of liquid–liquid two-phase flow at a horizontal T-junction. International Journal of Multiphase Flow, 33(2), 207-216.